



On the role of triethylene glycol in the preparation of highly active Ni-Mo/Al₂O₃ hydrodesulfurization catalysts: A spectroscopic study



Aída Gutiérrez-Alejandre^a, Geovani Laurrabaquio-Rosas^a, Jorge Ramírez^{a,*}, Guido Busca^b

^a UNICAT, Depto. de Ingeniería Química, Facultad de Química, Universidad Nacional Autónoma de México, Cd. Universitaria, México, DF 04510, Mexico

^b Laboratorio di Chimica delle Superfici e Catalisi, Dipartimento di Ingegneria Civile, Chimica e Ambientale, Università di Genova, Fiera del Mare, pad. D, I-16129 Genova, Italy

ARTICLE INFO

Article history:

Received 30 July 2014

Received in revised form 6 November 2014

Accepted 18 November 2014

Available online 25 November 2014

Keywords:

Triethylene glycol

Hydrodesulfurization

Infrared spectroscopy

ABSTRACT

The interaction of triethylene glycol (TEG) with alumina and its role in preparing improved NiMo/Al₂O₃ hydrodesulfurization catalysts was investigated by spectroscopic methods. The FT-IR study shows that TEG is mainly adsorbed on the corners and edges of the alumina microcrystals where the strongest Lewis sites and the higher ν OH frequency hydroxyl groups are mainly located. It is also observed that the Mo=O stretching vibration of surface molybdenyl groups in the oxide catalyst precursor is shifted down in the presence of TEG, indicating a lower interaction with the alumina surface. The IR spectra of CO adsorbed on the reduced/sulfided NiMo/Al₂O₃ catalysts confirm that the amount of promoted phase (NiMoS sites) increases in the samples prepared with TEG. Accordingly, the activity measurements in the HDS of 4,6-dimethylbenzothiophene show that the catalyst prepared with TEG is more active than the one prepared without it. It is proposed that TEG and its decomposition products, formed upon heating (mainly acetates) occupy preferably the strongly interacting edge and corner sites of the alumina crystals, forcing the Mo and Ni species to migrate mainly to the less reactive plane faces. This weakens the metal-support interaction allowing a better sulfidation and, at the same time, favoring the Ni–Mo interaction and the formation of the promoted NiMoS phase.

© 2014 Elsevier B.V. All rights reserved.

1. Introduction

The strict regulations in the content of sulfur in transport fuels calls for the design of highly active hydrodesulfurization (HDS) catalysts. Improved HDS catalysts based on Co- or Ni-promoted MoS₂ or WS₂-supported on alumina have been obtained, at least in part, thanks to the reformulation of the preparation procedure allowing to obtain better dispersion and higher levels of promotion. One of the methods to enhance the activity of HDS catalysts is through the use of organic additives. Among others, some patents cite triethylene glycol (TEG) as a useful additive in this respect [1–3].

Several studies have been published in the current literature concerning the effects of ethylene glycols to HDS catalysts but most of them concern the preparation of Co-Mo/Al₂O₃ catalysts [4–9]. As discussed by Costa et al. [9] different opinions are reported for the effect of TEG on the performance of Co-Mo/Al₂O₃ HDS catalysts. In particular, conflicting data are reported concerning the effect of the organic additive on the sulfidation behavior. It seems well

established that the additive hinders the interaction between the active phase precursors and alumina and that it enhances the dispersion of the Co and Mo species. As a consequence, more cobalt atoms are available to promote the MoS₂ crystallites formed during the sulfidation process. In contrast, the preparation of Ni-Mo/Al₂O₃ catalysts using glycols has been the object of less attention. Escobar et al. [10] studied the effect of increasing amounts of ethylene glycol (EG) on the preparation Ni-Mo-P/Al₂O₃ catalysts. From TPR experiments it was found that addition of ethylene glycol to the impregnating Ni–Mo solution resulted in a decreased interaction between the alumina support and the Ni and Mo phases. They also found that dispersion and sulfidability followed opposite trends when increasing the amount of EG; sulfidability decreased while dispersion of the Mo phases increased. Yin et al. [11] made a study on the impregnating solution and reported that by adding glycol, the presence of the $H_x[P_2Mo_5O_{23}]^{(6-x)-}$ heteropolycompound is favored over several other species. No references were found in the scientific literature for studies with NiMo catalysts using triethylene glycol as organic additive.

In the present work we perform a detailed IR spectroscopic study of Ni-Mo/Al₂O₃ catalysts prepared with and without TEG to understand the interaction of the additive with the support and

* Corresponding author. Tel.: +52 55 56225349

E-mail address: jrs@unam.mx (J. Ramírez).

active phases, and the changes induced by the organic additive on the structure, dispersion, and sulfidation of the Mo and Ni surface species. The results from the spectroscopic study will be used to explain the variations in the 4,6-dimethylbenzothiophene HDS activity of catalysts prepared with and without TEG.

2. Experimental

2.1. Catalysts preparation

Commercial γ -Al₂O₃ from Sasol with BET surface area of 212 m²/g was used as catalyst support.

The NiMoT/ γ -Al₂O₃ catalyst, denoted hereafter as NiMoT, was prepared by incipient wetness successive impregnation. First, the alumina support was impregnated with an aqueous solution of ammonium heptamolybdate ((NH₄)₆Mo₇O₂₄ 4H₂O) with the appropriate molybdenum content to obtain 2.8 Mo atoms/nm². After that, the solid was dried at 373 K during 24 h. The resulting powder was impregnated with an aqueous solution containing nickel nitrate (Ni(NO₃)₂·6 H₂O) and triethylene glycol in adequate proportions to maintain a Ni/(Ni + Mo) atomic ratio of 0.33 and a TEG/Ni molar ratio of 1.2 respectively. Finally, the impregnated sample was dried at 373 K during 24 h.

The conventional NiMo catalyst, without TEG, used as reference was prepared using the same procedure as for NiMoT but in this case, after the drying step; the solid was calcined at 673 K for 4 h.

An additional support sample of alumina impregnated with the same amount of TEG used for the NiMoT catalyst was prepared by impregnating the alumina support with an aqueous solution of triethylene glycol (C₆H₁₄O₄). After impregnation, the solid powder was dried at 373 K during 24 h.

2.2. Spectroscopic characterization

IR spectra were collected (100 scans, 4 cm⁻¹ resolution) using a Nicolet Nexus FT-IR instrument. Pure catalyst powder pressed disks were activated by outgassing at several temperatures, from room temperature up to 773 K, using an infrared cell connected to a conventional gas manipulation/outgassing vacuum line.

2.2.1. Pyridine adsorption

The adsorption of pyridine was performed by contacting a catalyst sample (wafer of \sim 10 mg/cm²), preactivated by outgassing at 573 K, with 1 Torr of pyridine vapor. After that the IR spectrum was collected.

2.2.2. CO adsorption on sulfided samples

For the CO adsorption experiments, a self-supporting wafer of \sim 7.5 mg/cm² of pure catalyst powder was placed in the IR cell, and sulfided at the same conditions as those used in the catalytic activity tests (673 K for 4 h in H₂S/H₂ mixture (15% v/v)). Subsequently, the cell was outgassed in vacuum at 723 K for 2 h. Then, CO adsorption at 100 K was performed by adding small pulses of CO up to a pressure of 1 Torr equilibrium. The spectra were taken with a Thermo Nicolet 6700 FTIR spectrophotometer using a resolution of 4 cm⁻¹ and 100 scans per spectrum. The integrated molar extinction coefficient of CO adsorbed on the sulfided catalysts was obtained by introducing several small doses of CO (0.005 Torr) in the IR cell at liquid nitrogen temperature (100 K). Turn over frequency (TOF) values were calculated from CO adsorption experiments. From this analysis, the number of active sites per gram of sulfided catalyst was estimated.

2.2.3. High resolution electron microscopy

HRTEM micrographs of the sulfided catalysts were obtained with a JEOL 2010 transmission electron microscope operating at

200 kV with 1.9 Å point to point resolution. Prior to the analysis, the samples were sulfided at the same conditions as for the catalytic activity tests. The sulfided samples were dispersed by ultrasonication in heptane for 20 min, and a drop of the supernatant liquid was placed on a holey carbon film supported on a copper grid. For the statistical analysis of the size and stacking distribution of MoS₂ crystallites, more than 300 crystallites were measured. From these measurements a value for MoS₂ dispersion was obtained by calculating the Mo_{edge}/Mo_{total} ratio assuming hexagonal MoS₂ crystallites [12].

2.2.4. UV-vis-DRS

Diffuse reflectance spectra were obtained at room temperature with a Perkin-Elmer JascoV-570 spectrometer equipped with an integration sphere.

2.3. Catalytic activity test

Prior to the catalytic test, the catalyst precursors were activated using 40 mL/min of a H₂S/H₂ mixture (15% v/v) at 673 K for 4 h. The catalytic activity tests were performed in a Parr batch reactor operating at 593 K and 1200 psig of hydrogen during 6 h. The reaction mixture contained 4,6-dimethylbenzothiophene (1000 ppm as S) in 40 mL of n-decane and 200 mg of sulfided catalyst. Samples were taken every 30 min during the first 3 h, then after each hour. The analysis of the reaction products was performed using an HP 6890 gas chromatograph, equipped with a flame ionization detector.

For the calculation of the rate constants for the disappearance of 4,6-DMDBT, an irreversible pseudo first order reaction rate was considered: $-r_{4,6\text{-DMDBT}} = kC_{4,6\text{-DMDBT}}$. The value of the overall rate constant was then obtained from the slope of the linear expression: $\ln(C_{4,6\text{-DMDBT}}/C_{4,6\text{-DMDBT Feed}}) = -kt$. Where k is the sum of $k_{\text{DDS}} + k_{\text{HYD}}$, k_{DDS} is the reaction rate constant for the hydrogenolysis route, k_{HYD} is the reaction rate constant for the hydrogenation route, and t is the reaction time.

The individual rate constants k_{DDS} and k_{HYD} were obtained from the value of the initial selectivity $k_{\text{HYD}}/k_{\text{DDS}}$ and the overall rate constant ($k = k_{\text{DDS}} + k_{\text{HYD}}$).

The $k_{\text{HYD}}/k_{\text{DDS}}$ ratio is given by the ratio of hydrogenated to hydrogenolysis products, as shown in the following equation:

$$\frac{k_{\text{HYD}}}{k_{\text{DDS}}} = \frac{[\text{TMDMBT} + \text{HMDMBT} + \text{MCHT} + \text{DMDCH}]}{[\text{DMDF}]}$$

where

TMDMBT = tetrahydrodimethylbenzothiophene,
HMDMBT = Hexahydrodimethylbenzothiophene,
MCHT = Methylcyclohexyltoluene, DMDCH = Dimethyldicyclohexyl
and DMDF = Dimethylbiphenyl.

3. Results and discussion

3.1. Catalytic activity

The results for NiMoT and NiMo catalysts are summarized in Table 1. The data show that NiMoT, prepared using TEG, is about 2.4 times more active than the catalyst prepared without TEG. Accordingly, the rate constant for the direct desulfurization route (DDS) increased 1.63 times and that for the HYD route 2.85 times. The HYD/DDS ratio was 7.9 for NiMoT whereas it was only 4.5 for NiMo.

Since the DDS takes place in coordinatively unsaturated sites on the edges of the NiMoS phase, the increase in DDS indicates an improvement in the active phase dispersion. On the other hand, an enhanced transformation through the HYD route, that takes place mostly in the BRIM sites located on the top basal plane of the MoS₂ crystallites [13], signals a better sulfidation of the active phase.

Table 1

Table 1 Catalytic activity in the hydrodesulfurization of 4,6-dimethylbenzothiophene ($T = 593$ K and 1200 psig), and dispersion for the prepared catalysts.

Catalyst	k (L/h g _{CAT})	k_{DDS} (L/h g _{CAT})	k_{HYD} (L/h g _{CAT})	$k_{\text{HYD}}/k_{\text{DDS}}$	TOF $\times 10^4$ (h ⁻¹)	Dispersion
NiMo	0.088	0.016	0.072	4.5	1.9	0.31
NiMoT	0.232	0.026	0.205	7.9	4.6	0.35

The significant rise in HDS activity obtained using TEG (2.6 times) cannot be fully explained by the HRTEM observations that show 13% increase in MoS_2 dispersion of the sample NiMoT respect to NiMo. Therefore, to understand better the observed changes in activity, an IR study of the interactions of TEG with the alumina support and the catalyst (before sulfidation) was undertaken.

3.2. IR study of the interaction of TEG with alumina

In Fig. 1a the infrared spectra of alumina with TEG, γ -Al₂O₃-TEG, recorded after outgassing at increasing temperatures, from room temperature to 773 K, are reported. The spectrum of pure γ -Al₂O₃ outgassed at 773 K is also reported for comparison. In this figure, adsorbed TEG species are responsible for the presence of several bands, which are not present in the spectrum of pure γ -Al₂O₃. These bands are more evident in the subtraction spectra (where the spectrum of pure alumina is subtracted), shown in Fig. 1b, where the IR bands can be compared with those of pure liquid TEG deposited on a KBr disk. In Fig. 1a, the strong bands in the 3000–2700 cm⁻¹ region are associated to C-H stretching vibrations, ν_{CH} . In the region below 1500 cm⁻¹, the bands observed at 1454, 1350, 1299, 1251, 1113 and 1079 cm⁻¹ corresponding to δCH_2 , δCOH , γCH_2 , τCH_2 and two different νCO vibrations respectively, are associated to adsorbed TEG species [14]. The band at 1647 cm⁻¹ in the spectrum of liquid TEG (Fig. 1b) can be assigned to water impurities ($\delta\text{H}_2\text{O}$). Accordingly, the shoulder at 1630 cm⁻¹ in the γ -Al₂O₃-TEG spectrum at room

temperature can be associated to adsorbed water arising from the water impurities in TEG.

The spectrum of $\gamma\text{-Al}_2\text{O}_3$ -TEG shows, after outgassing at room temperature, a peak at 1598 cm^{-1} , which is not evident in the spectrum of TEG. This peak is associated to small amounts of carboxylate impurities, which are present in the spectrum of $\gamma\text{-Al}_2\text{O}_3$, and are likely due to the presence of residual organic impurities coming from the preparation method of Sasol aluminas (Ziegler process from aluminum alkoxides [15]).

In the OH stretching region the spectrum of γ -Al₂O₃-TEG shows, after outgassing at room temperature, a broad absorption centered near 3630 cm⁻¹ tailed towards lower frequencies. It is evident in Fig. 1a that the spectrum of γ -Al₂O₃-TEG gradually modifies with the outgassing temperature. The progressive disappearance of the broad shoulder near 1630 cm⁻¹ is observed when heating from 373 to 573 K. Correspondingly, a change in the shape of the absorption in the OH stretching region occurs. In fact the main maximum near 3630 cm⁻¹ disappears, while two components at \sim 3670 cm⁻¹ (sharp, weak) and at \sim 3550 cm⁻¹ become evident. This indicates that adsorbed water, responsible for the bands centered at 3630 and 1630 cm⁻¹ (ν OH's and δ H₂O, respectively), desorbs while the hydroxyl groups are still at the surface. Additionally, dehydroxylation of alumina as well as dissociation of the TEG's hydroxyl groups may occur, in agreement with a change in the shape of the absorption in the 1200–1000 cm⁻¹ range, due to C–O(H) vibrations.

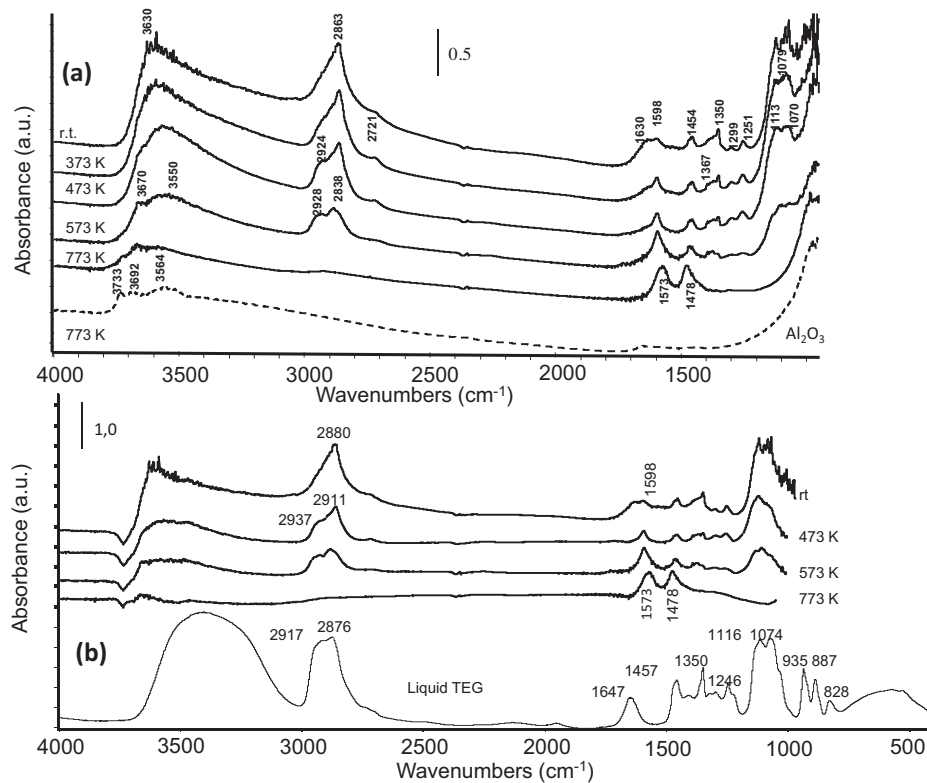


Fig. 1. (a) FTIR spectra for γ -Al₂O₃ (broken line) and γ -Al₂O₃-TEG (full line), after outgassing at several temperatures. (b) FT-IR spectra of liquid TEG + KBr mixture (full line) as reference, and subtraction spectra of γ -Al₂O₃-TEG (full line) after outgassing at several temperatures.

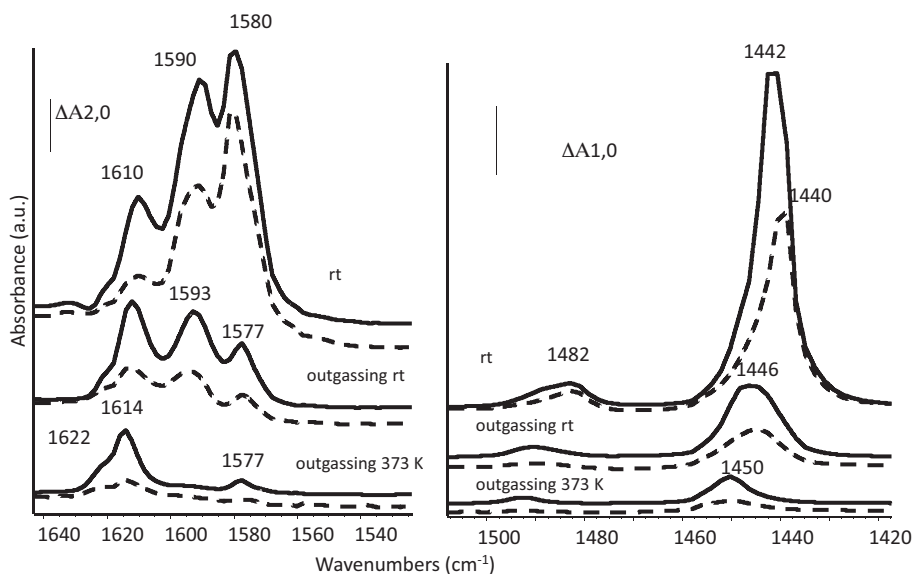


Fig. 2. Subtraction FTIR spectra of pyridine adsorbed on γ - Al_2O_3 (full lines) and γ - Al_2O_3 -TEG (broken lines), both pre-activated by outgassing at 473 K. The spectra are recorded in contact with pyridine vapor (top), after outgassing at r.t. (middle) and at 373 (bottom).

After outgassing at 773 K, the spectrum of γ - Al_2O_3 -TEG in the 3800–3500 cm^{-1} region (OH-stretchings) is significantly different from that of pure alumina activated in the same conditions. The spectrum of pure γ - Al_2O_3 , after heating at 773 K, shows the bands of surface free (non H-bonded) hydroxyl groups at 3733 and 3692 cm^{-1} , with possibly some additional weak component at higher frequency. A broad band at 3565–3500 cm^{-1} , due to H-bonded hydroxyl groups is also evident. In contrast, in the spectrum of γ - Al_2O_3 -TEG, after outgassing at 773 K, only very weak bands of free hydroxyls are observed. The subtractions reported in Fig. 1b confirm this; the spectra of γ - Al_2O_3 -TEG displays higher absorption than the pure γ - Al_2O_3 one in the region below 3650 cm^{-1} , indicating the presence of more H-bonded OHs. In line with this, the spectrum of γ - Al_2O_3 -TEG is weaker than that of γ - Al_2O_3 at higher frequencies in the region of free OHs (negative bands in the subtraction spectrum). This confirms that TEG species perturb or substitute free hydroxyl groups of alumina, while producing more H-bonded hydroxyl groups, either of the Al-OH or of the C-OH type. These data show that the adsorption of TEG indeed involves an interaction with the surface hydroxyl groups of alumina.

In the lower frequency region the spectrum is progressively modified. The shape of the strong CO stretching bands in the region, quite different from the corresponding bands in pure TEG, is modified by outgassing at 300–573 K. All the bands in the 1400–1000 cm^{-1} region diminish progressively and fully disappear at 773 K while two main bands become evident at 1573 and 1478 cm^{-1} , possibly with a component near 1400 cm^{-1} . The resulting spectrum after outgassing at 773 K corresponds to that of carboxylate species (COO asymmetric and symmetric stretchings, respectively), very likely acetate species adsorbed on alumina [16], coming from the decomposition of TEG.

The IR spectra thus show that TEG is stable on the surface, although likely partially converted to dissociated species, at least until 573 K, while it decomposes to acetate species above this temperature. Acetate species are still observed at 773 K. These results indicate that both TEG and acetate species interact with or even displace most of the free surface hydroxyl groups.

To reveal the modifications of the surface properties of γ - Al_2O_3 by adsorbed TEG, the IR spectra of pyridine adsorbed on both γ - Al_2O_3 and γ - Al_2O_3 -TEG, previously outgassed at 473 K, have also been investigated (Fig. 2).

As it is well known [17], the spectrum of pyridine presents in the 1800–1400 cm^{-1} region, four strong bands (ring vibrations) denoted as 8a, 8b, 19a and 19b modes, centered, in the liquid, at 1583, 1577, 1481 and 1436 cm^{-1} respectively. In particular, the 8a and 19b modes are both sensitive to interaction with Lewis sites, being shifted up with the strength of the adsorbing site.

The spectra of pyridine adsorbed on γ - Al_2O_3 and γ - Al_2O_3 -TEG have a remarkably different intensity, showing that the adsorbed amount of pyridine is significantly decreased (nearly 39% less) by the presence of TEG. Three definite bands observed in the 8a/8b region at ca 1610, 1590 and 1580 cm^{-1} are assigned to two 8a modes (at least two different adsorbed species) and the 8b mode of adsorbed pyridine respectively. An additional shoulder is evident at higher frequencies (ca 1622 cm^{-1}).

Before outgassing, bands at 1482 (weak) and 1442 cm^{-1} , due to the 19a and 19b modes of adsorbed pyridine are observed. The spectra of pyridine adsorbed on the two samples (γ - Al_2O_3 and γ - Al_2O_3 -TEG), show the presence of four different pyridine species. The bands at ca 1580 and 1440 cm^{-1} can be predominantly due to 8a and 19b modes of weakly bonded, likely H-bonded, pyridine species, which disappear by outgassing at room temperature. After outgassing at r.t. three different pyridine species still remain, characterized by two well resolved 8a bands at 1593 and 1612 cm^{-1} , and a shoulder at 1621 cm^{-1} . The band at 1577 cm^{-1} is due to the non-sensitive 8b mode of all three species. The bands associated to the 8a mode shift slightly to higher frequency while decreasing in intensity upon outgassing at increasing temperature.

The presence of at least three different Lewis sites on alumina has already been reported by many authors [15,18,19]. As expected, none of the solids present significant Brønsted acidity bands attributed to pyridinium ion.

The bands of pyridine adsorbed on Lewis sites on the two surfaces, before and after contacting with TEG, are located nearly at the same frequencies. However, the intensity of the bands associated to pyridine adsorbed on the strongest sites (8a band at 1614 cm^{-1} and shoulder at 1622 cm^{-1} , which are related to the 19b bands at 1460–1450 cm^{-1}) is 70% lower on γ - Al_2O_3 -TEG with respect to γ - Al_2O_3 than those due to physisorbed species and species bonded to weaker Lewis sites.

A thorough analysis of the available data from the literature [20] led us to conclude that pyridine, responsible for the 8a modes at 1614 and 1622 cm^{-1} , is interacting via a Lewis-type interaction

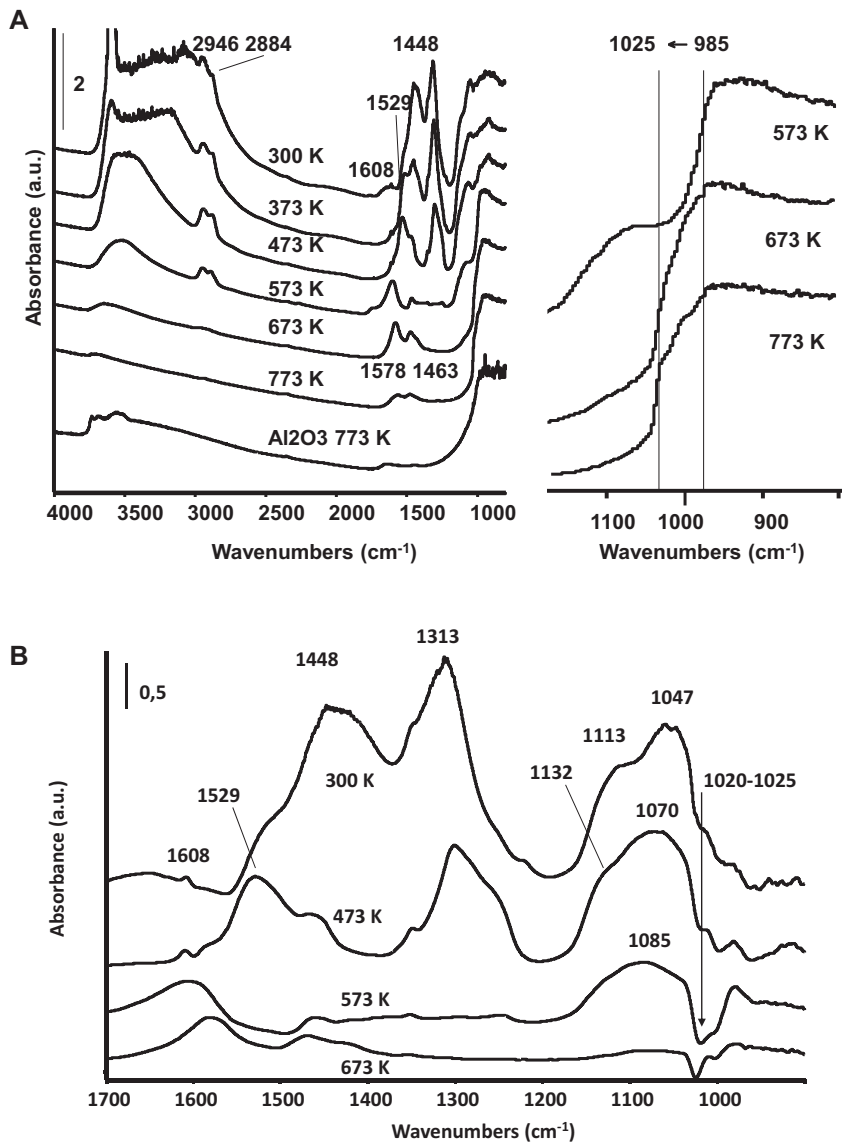


Fig. 3. (a) FTIR spectra for NiMoT after outgassing at increasing temperatures and Al_2O_3 support as reference. (b) FTIR subtraction spectra for NiMoT after outgassing at increasing temperatures. The spectrum recorded after outgassing at 773 K is subtracted from the others.

with Al^{3+} in coordination four, likely located on the edges, corners, or similar defects on the alumina crystal surface. A similar conclusion was obtained for OH's absorbing at higher frequencies that are likely bonded to tetracoordinated Al ions mainly located on edges and corners of the alumina crystals [17].

In summary, Figs. 1 and 2 suggest that TEG primarily interacts with the more exposed and strongest sites (Lewis sites and hydroxyl groups) of alumina, located in edges and corners, leaving the less exposed sites located on plane faces largely free.

The interaction of TEG with the alumina surface is evidently strong since adsorbed TEG decomposed only after heating above 573 K, before being desorbed. The interaction is also stronger than that of water, which is in fact desorbed in the 300–573 K range, when TEG is still stable on the alumina surface. In any case, the decomposition of adsorbed TEG at 773 K leaves on the surface carboxylate species, likely acetates, still interacting with corner and edge sites. Thus, taking into account the temperatures used for catalyst sulfidation and the reaction test, it could be considered that the use of TEG “irreversibly” poisons the strongest sites of alumina located on edges and corners.

3.3. IR study of the NiMoT catalyst precursor

In Fig. 3a, the IR spectra of the NiMoT catalyst precursor after outgassing at different temperatures are reported. In the right section of the figure, the 1200–800 cm^{-1} region of the spectra obtained after outgassing at 573–773 K was expanded. In Fig. 3b the subtraction spectra are reported in the 1700–900 cm^{-1} region; they were obtained by subtracting from each spectrum that of NiMoT after outgassing at 773 K.

The first spectrum in both figures refers to NiMoT dried at 300 K. The spectra in Fig. 3b show absorption bands at 1113 and 1047 cm^{-1} , due to CO stretchings of adsorbed TEG. After outgassing, the position of the band at 1047 cm^{-1} shifted to 1070 cm^{-1} , similarly to what was observed for the $\gamma\text{-Al}_2\text{O}_3$ -TEG sample. Similarly, in Fig. 3a, the CH stretching modes of adsorbed TEG are evident at 2946 and 2884 cm^{-1} .

The strong broad absorption in the region 3500–2700 cm^{-1} and the sharper one at 1448 cm^{-1} are due to ammonium ions (νNH_3^+ and $\delta_{\text{as}}\text{NH}_4^+$ respectively). In fact, these two features disappear by outgassing in the range 300–573 K, due to the decomposition of ammonium ions with evolution of gas phase ammonia. Traces of

adsorbed ammonia are associated to the weak band at 1608 cm^{-1} ($\delta_{\text{as}}\text{NH}_3$). The very strong band at 1313 cm^{-1} , more evident in Fig. 3b, is likely associated to the component observed in the range 1500 – 1530 cm^{-1} corresponding to bi-coordinated nitrate species. These features fully disappear at 573 K . After outgassing at higher temperature, 573 – 773 K , the spectra of NiMoT look very similar to those of $\gamma\text{-Al}_2\text{O}_3$ -TEG (shown in Fig. 1) in the region above 1050 cm^{-1} . The similarity of the NiMoT and $\gamma\text{-Al}_2\text{O}_3$ -TEG spectra in this region indicates that not significant chelation of Ni ions by TEG occurs, and that the primary interaction of TEG is with alumina.

In the lower frequency region ($<1050\text{ cm}^{-1}$), the spectra of the NiMoT catalyst show a sharp absorption, which is not present on the alumina sample. This absorption, evident as an edge in Fig. 3a, clearly shifts from near 985 cm^{-1} to near 1025 cm^{-1} when the samples are heated under vacuum above 473 K . Correspondingly, the subtractions reported in Fig. 3b show a negative band situated near 1021 cm^{-1} in all spectra. The position of this band is typical of the Mo=O stretching of surface molybdenyl species [20,21] on alumina. The observed shift from 985 to near 1025 cm^{-1} , when the samples are heated under vacuum above 473 K , could be associated to dehydration/deshydroxylation of the samples and the disappearing of van der Waals interactions between water molecules and Mo=O bonds [22,23]. However, according to Fig. 3a, this dehydration/deshydroxylation process occurs mainly below 473 K . Moreover, the shift observed in Fig. 3a by desorption of water is continuous and occurs at lower temperatures, whereas for TEG it is sudden and occurs at higher temperature.

Thus, the observed shift suggests that the presence of TEG causes a modification of the coordination state of molybdenum on alumina, and lowers the Mo=O molybdenyl bond order. According to the literature [21], a higher Mo=O frequency indicates lower basicity of the other ligands around molybdenum. Thus, the data reported here suggest that either TEG interacts directly with the molybdenyl ions, providing O-terminated ligands with lower basicity than alumina's oxide anions, or TEG shifts the molybdenyl ions to less acid–basic support sites.

On the alumina surface, the strongest acidic–basic sites are highly coordinatively unsaturated Al^{3+} cations (Lewis acidic sites) in tetrahedral environment, and oxide anions or hydroxyl species (basic sites) located on edges and corners of the $\gamma\text{-Al}_2\text{O}_3$ nanocrystals [15]. The overall FTIR results suggest that in the absence of TEG, $[\text{Mo=O}]^{n+}$ cations, with n likely = 4, will largely adsorb on the more acid–basic sites located on edges and corners of the alumina crystals, being characterized, in these conditions by the Mo=O stretching near 1025 cm^{-1} . Only when in excess they will also interact with the *plane alumina crystal faces*, where they can take the higher coordination characterized by Mo=O stretching at 985 cm^{-1} . In the presence of TEG, $[\text{Mo=O}]^{4+}$ ions will be forced to shift predominantly over plane alumina crystal faces, because the edge sites will be “poisoned” by TEG. The partial decomposition of TEG to acetates starting to occur (incompletely) above 473 K will progressively free part of the edge sites, where $[\text{Mo=O}]^{4+}$ ions can diffuse back. However, the decomposition of adsorbed TEG at 773 K leaves on the surface carboxylate species, likely acetates, still interacting with corner and edge sites. According to the temperatures used for catalyst sulfidation and reaction test, it could be considered that the use of TEG “irreversibly” poisons part of the strongest sites of alumina, located on edges and corners.

3.4. UV–vis–NIR DR study of the catalyst precursors

The UV–vis spectrum of the NiMo and NiMoT catalyst precursors recorded in air without any pretreatments, are compared in Fig. 4. They are also compared with the spectra of a conventionally

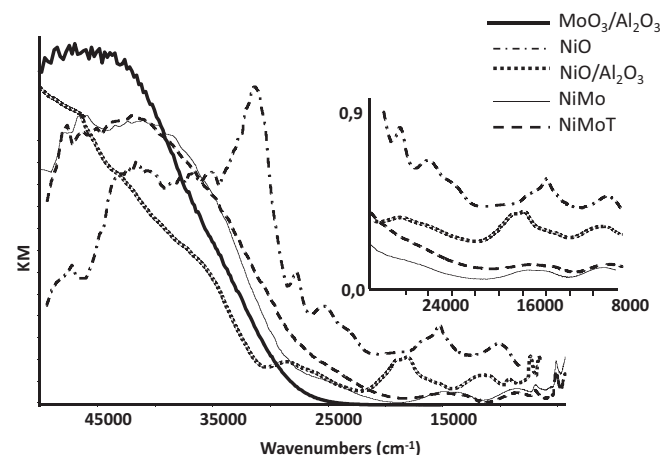


Fig. 4. UV–vis DR spectra at room temperature of catalysts before sulfidation.

prepared 5% NiO/Al₂O₃, and 8% MoO₃/Al₂O₃ in their oxide form, as well as with the spectrum of bulk nanometric NiO.

In all cases, the strong absorption region observed above $28,500\text{ cm}^{-1}$ is associated to charge transfer transitions (CTT) of the O^{2-} (2p) \rightarrow Mo^{5+} (3d) and/or O^{2-} (2p) \rightarrow Ni^{2+} (3d) that become essentially valence -to- conduction band transitions for finite bulk systems.

The spectrum of MoO₃/Al₂O₃ at low loading has been reported by several authors [24–26]. The strong CTT band is centered, as usual, at about $44,000\text{ cm}^{-1}$ ($\lambda = 230\text{ nm}$) in the case of hydrated “monomeric” molybdenyl species. The absorption decreases continuously at lower wavenumbers and becomes negligible just at the limit of the visible region, near $25,000\text{ cm}^{-1}$.

The spectrum of the NiMo sample presents the strong absorption maximum at ca $41,000\text{ cm}^{-1}$ possibly with a second maximum at ca $46,300\text{ cm}^{-1}$ (216 and 244 nm), while the spectrum of NiMoT shows its main maximum at $41,800\text{ cm}^{-1}$ (240 nm), possibly with a second component, not clearly defined because of the noise present near the limit of 200 nm of the UV source of the instrument.

For highly dispersed Ni^{2+} on alumina the absorption grows towards higher energies, the maximum being above $45,000\text{ cm}^{-1}$ (below 220 nm).

As reported previously by Garbarino et al. [27], by increasing the amount of Ni^{2+} on alumina first a strong absorption appears at $37,000\text{ cm}^{-1}$, assigned to very small NiO particles, then the spectrum of bulk NiO appears, with an almost continuous absorption with two maxima at $30,000$ and $41,500\text{ cm}^{-1}$, at very high Ni loadings [27]. Since we do not observe the contributions of Ni^{2+} species in this region it seems quite reasonable to attribute the main maxima observed in the region $46,000$ – $40,000\text{ cm}^{-1}$ predominantly to the O^{2-} (2p) \rightarrow Mo^{5+} (3d) CT transition. The presence of Ni^{2+} is evidenced by the broadening of the low energy tail of the CT absorption, shifting towards the visible region, influenced by the O^{2-} (2p) \rightarrow Ni^{2+} (3d) CT transitions where, however, other d-d components of Ni^{2+} also exist.

In the lower wavenumbers region, below $28,500\text{ cm}^{-1}$, the d-d transitions of Ni^{2+} are expected, the spectra of the NiMo catalysts are very similar to each other and different from those of dispersed NiO/Al₂O₃ and NiO, suggesting that the TEG additive does not perturb the Ni species significantly.

The difference between the spectra of NiMoT and NiMo catalyst seems to be mostly in the shape of the strongest band, in the UV region with the threshold limit shifting to the visible region and the main maximum shifting slightly in the reverse sense. It seems likely that the presence of TEG increases the perturbation of Mo species, with a slight shift of the maximum and a broadening of the lower

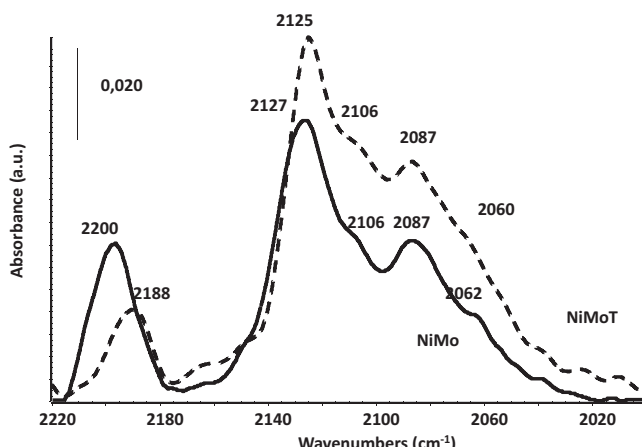


Fig. 5. IR spectra of CO adsorbed (1 Torr equilibrium) over NiMo (full line) and NiMoT (broken line) catalysts.

wavenumber tail of the O^{2-} (2p) \rightarrow Mo^{5+} (3d) CT transition, indicating an increase in the hexacoordinated Mo octahedral species.

According to the IR and UV-vis data discussed above, which indicate that the presence of TEG at the surface implies a lower frequency for the surface Mo=O stretching modes, we can conclude that TEG influences the state of molybdenum, forcing it towards a different position or coordination state where the interaction with nickel is increased. This would support that TEG shifts the Mo ions, at least in part, from edges and corners to plane alumina crystal faces.

3.5. IR spectra of adsorbed CO on sulfided NiMo catalysts

Fig. 5 displays the IR spectra of CO adsorbed at low temperature on the sulfided NiMo and NiMoT catalysts. The spectrum of NiMo agrees with that reported in the literature [28]. The main band at 2125 cm^{-1} is attributed to CO interacting with Ni^{2+} on the Ni-promoted MoS_2 phase, while the shoulder near 2060 cm^{-1} is attributed to CO adsorbing on Mo sites located near Ni ions in the same active phase. The absorption centered at 2106 and 2087 cm^{-1} should instead be associated to CO on non-promoted MoS_2 and NiS_x sites respectively. The still strong band at 2200 cm^{-1} , which has a shoulder at 2212 cm^{-1} , is associated to highly acidic Al^{3+} located in the edges and corners of the alumina crystals. Additionally, we can remind that unreduced/unsulfided Mo species does not adsorb CO being thus silent in this technique.

The spectrum of NiMoT is similar but shows stronger bands due to CO interacting with the NiMo sulfided species. A definite difference is observed in the region 2220 – 2170 cm^{-1} , where the band at 2200 – 2212 cm^{-1} is no more evident while a band at 2188 cm^{-1} is observed. This result confirms that TEG or its residuals such as acetate ions specifically interact with the strongest Al^{3+} ions, likely lowering their acidity. The definite change in the ratio between the band due to CO on NiMo sulfided species and that of CO on Al^{3+} on corners and edges would confirm that TEG favors an increased formation of the promoted NiMo sulfide species by avoiding the interaction of Mo with strongly interacting OH's located on edges and corners of the alumina support, and thus promoting an increased interaction of Mo with Ni on the plane alumina crystal faces.

The results from the catalytic activity tests show that the NiMoT catalyst is 2.6 times more active than NiMo/ Al_2O_3 . The IR data suggest on the other hand that TEG is adsorbed strongly on alumina, where it starts to decompose, in dynamic vacuum, only above 573 – 673 K , leaving on the surface even more stable acetate species. The IR data also show that the presence of TEG influences

the state of molybdenyl species, whose Mo=O stretching frequency is observed at lower frequency (985 cm^{-1}) than when TEG is absent (1025 cm^{-1}), or start to be partly decomposed. Additionally, the UV-vis data indicate that the presence of TEG does not modify significantly the d-d transitions of Ni^{2+} , while shifting and broadening to lower wavenumbers the charge transfer transition region, where the O^{2-} (2p) \rightarrow Mo^{5+} (3d) CT transition is predominant. It is consequently concluded that the presence of TEG influences the structure and/or the location of surface molybdenyl species inducing a greater interaction with the Ni species.

A possible interpretation, based on previous data concerning multiple impregnations of oxides on oxide [29], is the following: metal ionic species, when interacting at the surface of metal oxides such as alumina, behave in relation to their acidic–basic nature. Both Ni^{2+} and $[Mo=O]^{4+}$ (molybdenyl) ions are Lewis acidic in nature and will compete with each other for the interaction on the most basic sites of the alumina surface. However, to preserve neutrality, their charge has to be compensated by (oxide or hydroxide) anions that will also adsorb on the support surface. The ionic pairs will interact with the most exposed acid–base pairs of the support surface.

Spectral data indicate (e.g. adsorption of pyridine on molybdena-based solids and Ni^{2+} -containing solids) that molybdenyl species with their paired anions are more ionic than Ni^{2+} ions and their corresponding anions. Thus molybdenyl species will interact with the strongest acidic–basic sites of the alumina surface forcing the Ni^{2+} ions to shift over to weaker acidic–basic surface sites. This is the reason why the d-d Ni^{2+} transitions for NiO/Al_2O_3 are very different from those observed in $NiMo/Al_2O_3$ species.

However, TEG (as any alcohol) adsorbs on alumina over Lewis acid sites through its oxygen lone pair [30]. Thus, TEG is able to shift surface molybdenyl species from the strongest acidic–basic sites of alumina, to weaker ones, where their interaction with Ni can become more likely. It seems quite reasonable to suppose that the strongest acidic–basic sites of the alumina surface are on the surface defects (edges and corners, or steps, over the surface of the alumina microcrystals). Thus TEG will shift the molybdenyl species from the surface defective sites forcing them to migrate to plane crystal faces, where the interaction with alumina is weaker and interaction with nickel may be easier. The location of both Mo and Ni species on the plane faces favors their interaction, that is, the formation of Ni–Mo species that will contribute to the formation of a well promoted Ni–Mo–S phase; the lower interaction with the alumina surface in plane crystal faces can be lowered even more by the interaction of TEG with the alumina surface; this will favor a better sulfidation of the Mo species. This explanation is consistent with the observed formation of heteropolycompounds in the case of $CoMoP/Al_2O_3$ catalysts prepared using a glycol compound [5,6,9].

4. Conclusions

The interaction of triethylene glycol (TEG) with alumina and its role in preparing improved NiMo/ Al_2O_3 hydrodesulfurization catalysts has been investigated by spectroscopic methods. From the results of the study we can say that, at the reaction conditions used in our experiments, the catalyst prepared with TEG is 2.4 times more active in the HDS of 4,6-dimethylbenzothiophene than a similar catalyst prepared without the additive and following the conventional method of impregnation, drying, calcination, and sulfidation. The higher activity of the catalyst prepared with TEG can be explained because:

- TEG adsorbs mainly on the corners, edges, and other defects of the alumina microcrystals, where the strongest Lewis sites and the higher νOH frequency hydroxyl groups are mainly located.

- TEG and their decomposition products, formed upon heating (mainly acetates) occupy the strongly interacting edge and corner sites of the alumina crystals, forcing the Mo and Ni species to migrate to the less interacting plane faces of the alumina surface. This weakens the metal-support interaction allowing a better sulfidation and favoring at the same time the Ni–Mo interaction and consequently, the formation of increased amounts of the promoted NiMoS phase.
- TEG does not modify significantly the d–d transitions of Ni^{2+} but it shifts and broadens the charge transfer transition region, where the $\text{O}^{2-}(2p) \rightarrow \text{Mo}^{5+}(3d)$ CT transition is predominant. Therefore, TEG does not modify the electronic structure of Ni but it does so with Mo. This suggests that TEG interacts preferable with edges and corners of the alumina support particles, where Mo is preferable deposited. The addition of TEG does not seem to modify the anchoring site of the Ni oxide precursor.
- The IR study of CO adsorbed on the reduced/sulfided NiMo catalysts confirm that the amount of sulfide phase increases in the samples prepared with TEG, indicating that TEG induces a better sulfidation of the oxide precursors, favoring the formation of the more active well sulfided type II NiMoS sites.

Acknowledgments

The authors acknowledge funding from Italy (MAE)-Mexico (CONACyT) exchange program, and to DGAPA-UNAM program through the PAPIIT IN-114112 project grant. I. Puente-Lee is acknowledged for the HRTEM work.

References

- [1] Patent EP 0601722 B1, (1994) Sumitomo Metal Mining Company.
- [2] Patent EP 1418002 A2, (2004) Sumimoto Metal Mining Company.
- [3] Patent EP 1418002 A3, (2012) Nippon Ketjen Company.
- [4] N. Iwamoto, A. Kagami, J. Lino, J. Jap. Petrol. Inst. 48 (4) (2005) 237–242.
- [5] D. Nicosia, R. Prins, J. Catal. 229 (2005) 424–438.
- [6] D. Nicosia, R. Prins, J. Catal. 231 (2005) 259–268.
- [7] V. Costa, K. Marchand, M. Digne, C. Geantet, Catal. Today 130 (2008) 69–74.
- [8] T. Son Nguyen, S. Loridant, L. Chantal, T. Cholley, C. Geantet, Appl. Catal. B: Environ. 107 (2011) 59–67.
- [9] V. Costa, B. Guichard, M. Digne, C. Legens, P. Lecour, K. Marchand, P. Raybaud, E. Krebs, C. Geantet, Catal. Sci. Tech. 3 (2013) 140–151.
- [10] J. Escobar, M.C. Barrera, J.A. Toledo, M.A. Cortés-Jácome, C. Angeles-Chávez, S. Nuñez, V. Santes, E. Gómez, L. Díaz, E. Romero, J.G. Pacheco, Appl. Catal. B: Environ. 88 (2009) 564–575.
- [11] H. Yin, T. Zhou, Y. liu, Y. Chai, C. Liu, J. Fuel Chem. Technol. 39 (2) (2011) 109–114.
- [12] E. Payen, R. Hubaut, S. Kasztelan, O. Poulet, J. Grimblot, J. Catal. 112 (1994) 123–132.
- [13] H. Topsøe, Appl. Catal. A: Gen. 322 (2007) 3–8.
- [14] O.B. Zubkova, A.N. Shabdash, J. Appl. Spectr. 14 (1971) 639–643.
- [15] G. Busca, Catal. Today 226 (2014) 2–13.
- [16] M.A. Peluso, E. Pronsato, J.E. Sambeth, H.J. Thomas, G. Busca, Appl. Catal. B: Environ. 78 (2008) 73–79.
- [17] M.I. Zaki, M.A. Hasan, F.A. Al-Sagheer, L. Pasupulety, Colloid. Surf. A: Physicochem. Eng. Aspects 190 (2001) 261–274.
- [18] T. Khoa Phung, A. Lagazzo, M.Á. Rivero Crespo, V. Sánchez Escribano, G. Busca, J. Catal. 311 (2014) 102–113.
- [19] T. Khoa Phung, C. Herrera, M.Á. Larrubia, M. García-Díéguez, E. Finocchio, L.J. Alemany, G. Busca, Appl. Catal. A: Gen. 483 (2014) 41–51.
- [20] G. Busca, J.C. Lavalley, Spectr. Acta 42A (1986) 443–445.
- [21] G. Busca, J. Raman Spec. 33 (2002) 348–358.
- [22] S.S. Chan, I.E. Wachs, L.L. Murrell, L. Wang, W. Keith Hall, J. Phys. Chem. 88 (1984) 5831–5835.
- [23] H. Jezirowski, H. Knözinger, J. Phys. Chem. 83 (1979) 1166–1173.
- [24] J. Ramirez, L. Cedeño, G. Busca, J. Catal. 184 (1999) 59–67.
- [25] M.A. Larrubia, G. Busca, Mater. Chem. Phys. 72 (2001) 337–346.
- [26] D. Nikolova, R. Edreva-Kardjieva, M. Glurginca, A. Meghea, J. Vakros, G.A. Voyatzis, C. Kordulis, J. Vib. Spectrosc. 44 (2007) 343–350.
- [27] G. Garbarino, S. Campodonico, A. Romero Perez, M.M. Carnasciali, P. Riani, E. Finocchio, G. Busca, Appl. Catal. A: Gen. 452 (2013) 163–173.
- [28] A. Travert, C. Dujardin, F. Maugé, E. Veilly, S. Cristol, J.-F. Paul, E. Payen, J. Phys. Chem. B 110 (2006) 1261–1270.
- [29] G. Ramis, G. Busca, F. Bregani, Catal. Lett. 18 (1993) 299–303.
- [30] G. Busca, P.F. Rossi, V. Lorenzelli, M. Benaissa, J. Travert, J.C. Lavalley, J. Phys. Chem. 89 (1985) 5433–5439.